Production and Weathering Exposure of Thermochromic Coatings Used as Sensors to Protect Electricity Distribution Systems

Ênio Brogni[a], Rodrigo da Costa Duarte[a], Rodrigo Cercená[a], Emerson Colonetti[a], Michael Peterson[b],

Maykon Cargnin[b], Alexandre Gonçalves Dal-Bó[a]* ![ORCID]

[a]Universidade do Extremo Sul Catarinense (UNESC), Programa de Pós-Graduação em Ciência e Engenharia de Materiais (PPGCEM), Laboratório de Processamento de Polímeros Avançados (LAPPA), 88806-000, Criciúma, SC, Brasil.
[b]Universidade do Extremo Sul Catarinense (UNESC), Programa de Pós-Graduação em Ciência e Engenharia de Materiais (PPGCEM), Laboratório de Reatores e Processos Industriais (LABREPI), 88806-000, Criciúma, SC, Brasil.

Currently, the overheating detection of electric system components is performed using thermal imaging devices, which depend on on-site regulation parameters, require skilled operators and suitable weather conditions. The development and application of innovative technologies to monitor hotspots has highlighted the use of sensors based on thermosensitive materials. In this study, a temperature sensor with thermochromic coating was developed. Thermochromic sensors covered with a varnish layer and nano-titanium oxide, in addition to thermochromic paint, were produced. A 2^3 experimental design was established to assess the performance of thermochromic sensors under artificial weathering conditions. Color measurements of the coatings were performed using the CIELAB method. Fourier-transform infrared (FTIR), UV-Vis (Ultraviolet-Visible), (thermogravimetric TGA, and Differential Scanning Calorimetry (DSC) analyses were performed on the sensors exposed to photodegradation to detect changes in the thermochromic coatings. The sensors exposed to thermodegradation, and salt spray weathering showed ΔE (total color difference) values below 1.50 points in the presence of TiO_2. In comparison, the sensors exposed to photodegradation showed ΔE values above 10 points, and UV-Vis analysis revealed changes in the chemical structure of the coatings. These results demonstrate that the varnish layer and TiO_2 can help minimize the degradation effects of temperature, light, and salinity.

Keywords: *Thermochromic sensor, Pigment, Thermochromic dye, Weathering.*

1. Introduction

Electricity distribution systems consist of several components that must transfer energy without interruption. These systems include electrical conductors, transformers, disconnecting switches, wedge-type connectors, and insulators, all of which play important roles in the operation of the system[1-4]. Problems caused by improper assembly, component aging, pollutant deposition, and oxidation can lead to dielectric breakdown or leakage currents. An increase in the electrical resistance of a connection results in energy dissipation due to the Joule effect, causing a temperature change[4]. The preventive maintenance of these electrical connections is usually accomplished by monitoring the temperature changes to avoid system outages. The use of thermography for temperature measurements and diagnostics is a well-established practice in preventive maintenance programs[5]. However, this method has several uncertainties that can lead to errors. Thus, the development of new materials and devices for fault identification is necessary[2].

Sensors can be constructed using a wide variety of materials and employ diverse detection and response techniques[3].

Reversible thermochromic composites consisting of a leuco dye, a color developer, and a solvent are characterized by coloration in the solid state and discoloration in the molten state. These color changes are due to modifications that occur in the structure of the compounds with changes in temperature[6-9].

Leuco dyes have two forms: a colored form and a colorless one Leuco dyes such as crystal violet lactone and its analogs have been well documented in the literature[10-13]. Fluoran dyes are a family of leuco dyes widely used in engineering design, biochemical analysis, light-emitting probes, and printing inks, and show good sensitivity and thermochromic stability[6,7,14].

Fluoran and crystal violet lactone dyes are pH sensitive. The ring opening of colorless lactones occurs via protonation by a weak acid (color developer), forming a colored phase. 2′-Anilino-6′-(dibutylamino)-3′-methylfluoran (ODB-2) dye has been assessed in thermochromic applications[14,15]. Bisphenol A (BPA) is a techno-commercial choice for color developers because it produces vivid colors and high-contrast changes[16].

*e-mail: adalbo@unesc.net

The color-transition mechanism of the ODB-2–BPA system is shown in Figure 1. In this thermochromic system, the color developer (ODB-2) is an electron-donating compound, whereas the color developer (bisphenol-A) acts as a proton donor to induce the color form of the leuco dye component. When the lactone ring of the color developer closes, the thermochromic compound exists in a colorless form. The addition of a proton induces the ring to open, leaving the dye in its colored form[6,10].

Low-melting-point fatty acids, amides, and alcohols such as stearyl alcohol are the most frequently used solvents for the production of thermochromic pigments. The colored former, developer, and solvent are melted and cooled to form colored pigment[10,11]. The mixture is then encapsulated for commercial use[11,15].

Encapsulated thermochromic pigments have been suggested to be applicable for use as thermochromic paints for painting components used in electricity distribution systems[17]. However, these components are typically exposed to different types of weathering, which can cause degradation.

Materials constituting paint may undergo degradation, which leads to changes in their mechanical, optical, or electrical properties[18,19]. The combination of several factors, such as the chemical and molecular structures, composition, and conditions of use, influences the degradation of a material. The most common chemical processes leading to coating degradation are photoinitiated oxidation and hydrolysis resulting from exposure to sunlight, air, and water. These processes are interrelated; for example, photo-oxidative degradation is intensified in environments with high humidity and heat[20]. Leuco dyes such as fluoran are poorly resistant to photodegradation[21,22]. The stability of leuco dyes depends on environmental factors such as the substrate and the presence of oxygen and water[21]. Structural modifications of fluoran dyes can significantly alter their resistance to photodegradation[22]. The addition of Zn (Zinc) or Ni (Nickel) salts to 1-hydroxy-2-naphthoic acid improves the photodegradation resistance of leuco dyes[23]. Polymorphs of TiO_2 (anatase and rutile) have shown good protection in polymeric materials exposed to accelerated weathering[24]; however, the ability of these materials to protect against leuco dyes has not been assessed.

This study aims to devise a thermochromic sensor for use in "naked-eye" monitoring of temperature variations in electricity distribution systems to identify hot spots in electrical connections caused by faults. To this end, a thermochromic coating was developed by adding the leuco pigment ODB-2 to alkyd paint. A microencapsulated reversible thermochromic pigment (ODB-2-BPA) was mixed with an alkyd paint and applied to aluminum substrates (electrical connectors).

To date, no studies have investigated the degradation resistance of thermochromic coatings using ODB-2-BPA encapsulated pigments. As these sensors were exposed to the environment, tests were performed to assess their degradation against artificial weathering due to salt spray, ultraviolet radiation, and thermal degradation.

In one set of tests, nanoscale titanium dioxide (TiO_2) was added to the paint formulation to improve the weathering resistance of the thermochromic coatings. In another series of tests, a protective varnish layer (VL) was applied to the thermochromic coating. In the third set of tests, the sensors were painted with TiO_2 and then VL was applied. The sensor with the best performance was determined using a 2^3 factorial experimental design, as well as ΔE assessment, FTIR and UV-vis spectroscopy, thermogravimetric analysis (TGA), and differential scanning calorimetry (DSC).

2. Materials and Methods

2.1. Materials

The materials used in this study were nano-titanium oxide TiO_2 nanopowder, 21 nm primary particle size (determined using TEM, $\geq 99.5\%$ purity, trace metals basis),
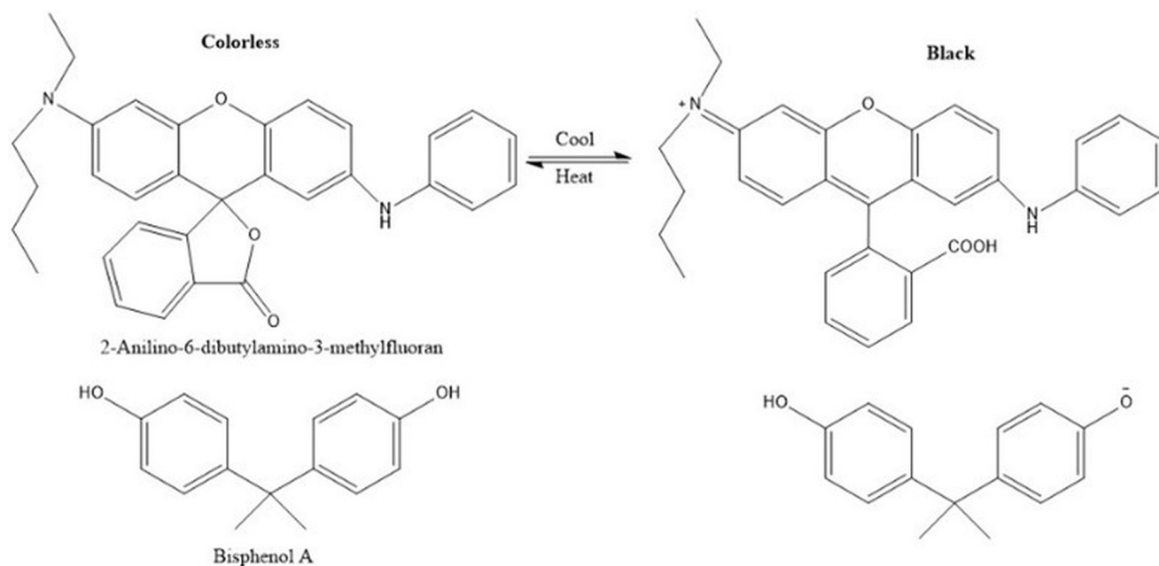

Figure 1. Schematic of the thermochromic mechanism of the ODB-2–BPA system. Adapted from Zhu et. al.[6].

Potassium bromide KBr (FT-IR grade, ≥99% purity, trace metals basis), n-Hexane ($CH_3(CH_2)_4CH_3$ HPLC grade, ≥97.0% purity (GC)) and Sodium chloride (NaCl, ACS reagent, ≥99.5% purity) were acquired from Sigma–Aldrich (St. Louis, MO, USA). Colorgin colorless spray varnish (Sherwin-Williams), thinner (Sherwin-Williams Automotiva Lazzuril), Gold Yellow (YAP) alkyd paint (Resicolor Indústria de Produtos Químicos Ltda), ODB-2 and BPA-based reversible black (65 °C) microencapsulated thermochromic pigments (MTP) product number HLR-7008 (Changzhou Hali Chemical Co., Ltd., Wujin, Changzhou, Jiangsu, CN). All reagents were of commercial grade and were used as received.

The substrates on which the thermochromic dyes were applied were red-series wedge connectors containing 99.9% Al (code CADC-102, Intelli Indústria de Terminais Elétricos, Ltd.).

2.2. Factorial experimental design

A 2^3 factorial design was established to obtain and analyze the performance of the thermochromic coatings against artificial weathering. The factors assessed were VL (with and without), TiO_2 (percentage ratio of 0% and 1% wt. %), and exposure time (ET) to weathering (240 h and 480 h). The proposed design is presented in Table 1. Each experiment was performed in triplicate according to this design. Experiments 1 and 5 involved mixtures of YAP and MTP (YAPMTP) subjected to ETs for 240 h and 480 h, respectively. Experiments 2 and 6 involved YAPMTP with VL subjected to ETs for 240 h and 480 h, respectively. Experiments 3 and 7 involved YAPMTP with TiO_2 (YAPMTP-TiO_2) subjected to ETs values of 240 and 480 h, respectively. Experiments 4 and 8 involved YAPMTP with TiO_2 and VL (YAPMTP-TiO_2-VL) subjected to ETs for 240 and 480 h, respectively.

2.3. Paint and thermochromic coating preparation

YAPMTP was prepared by mixing YAP with MTP and hexane solvent in a ratio of 71.5:11:17.5, w/w. The mixture was continuously stirred with a mechanical stirrer from the Fizatom, model 713D at 300 rpm for 2 h at 25 °C. After complete homogenization, the mixture was passed through a sieve (Würth do Brasil) with a synthetic wire mesh and electrostatic charge to remove particles larger than 8 μm.

The mixture was mechanically stirred YAPMTP-TiO_2 was prepared by adding 1 wt. % nano TiO_2 to the YAPMTP mixture. The mixture was stirred with a mechanical stirrer (Fizatom 713D) at 300 rpm for 2 h at 25 °C and sieved under the same conditions used to prepare YAPMTP. The thermochromic dyes, YAPMTP and YAPMTP-TiO_2 were stored in closed containers until use. The connectors to which the thermochromic paints were applied, were cleaned with a WD-40® SPECIALIST degreasing/detoxifying solution to remove surface oils.

The thermochromic paints and varnish were applied using a paint gun (Steula BC75-17, type HVLP: high volume low pressure) with a nozzle opening of 1.7 mm, 600 mL polypropylene cup, and a working pressure of 40 psi (275790 Pa) adjusted by an air flow regulator (Intech Machine-RA250). Thereafter, the thermochromic paints were cured under ambient conditions for 4 h, applied with a protective layer of Colorgin colorless spray varnish (Sherwin-Williams), and cured under ambient conditions for 24 h before conducting the experiments.

The thermochromic coatings prepared by mixing YAP with MTP were dark green at room temperature. When the temperature of the surface of the substrates on which the coatings were applied was increased to 65 °C, the painted surfaces turned yellow because the MTP changed from black to transparent at this temperature.

All paints were cured for 24 h under ambient conditions prior to characterization.

2.4. Exposure to artificial weathering

The performances of the developed thermochromic coatings (YAPMTP, YAPMTP-VL, YAPMTP-TiO_2, and YAPMTP-VL-TiO_2) were assessed in terms of their resistance to three types of artificial weathering: salt spray, thermodegradation, and photodegradation (Ultraviolet-A (UV-A) and Ultraviolet-B (UV-B)).

The salt-spray resistance test was performed in a corrosion chamber from Bass Equipamentos Ltd. (USC-MP-02/2006), following ASTM B117[25]. A 5 wt. % NaCl salt solution with a pH between 6 and 7 was used. The steam temperatures were 35 ± 2 °C (in the chamber) and 49 ± 2 °C (at the top of the air saturation tower) with a mist pressure of 117.68 ± 19.61 kPa.

Table 1. Data matrix of the 2^3 factorial design.

Run	Levels			Factors		
				VL	TiO_2 (%)	ET (h)
1	-1	-1	-1	Without	0	240
2	1	-1	-1	With	0	240
3	-1	1	-1	Without	1	240
4	1	1	-1	With	1	240
5	-1	-1	1	Without	0	480
6	1	-1	1	With	0	480
7	-1	1	1	Without	1	480
8	1	1	1	With	1	480

The thermodegradation test was performed by placing the samples in a Quimis vacuum chamber oven, model Q319V2, with vacuum system (off) heated to 50 ± 2 °C at atmospheric pressure. After exposure, the samples were removed from the oven, cooled to room temperature, and subjected to the required measurements.

Photodegradation tests were performed by subjecting the thermochromic coating samples to UV-A and UV-B radiation in a UV radiation chamber according to ASTM G154-16[26] in a thermal chamber manufactured by Biopar Equipamentos Eletrônicos Ltd. (model S22 SD). UV radiation was emitted by four tubular fluorescent lamps (Glight): two lamps emitted UV-A radiation (365 nm), and two lamps emitted UV-B radiation (315 nm) (total power 15 Watts (W)). The average radiation intensity was 8.54 W m^{-2}. Radiation measurements were performed in the chambers using a digital UV measurement device manufactured by Instrutherm (model MRUR-202). The chamber was not cooled, and the heating generated by the bulbs reached 45 ± 2 ºC.

2.5. Characterizations

The stability of the dyes was monitored visually and using zeta-potential (ζ) measurements, which were carried out in a NanoBrook Omni (Brookhaven Instruments Corporation, Holtsville, NY, USA) with Standard Laser 40 mW red diode laser, using a Phase Analysis Light Scattering (PALS) technique, with mobility range 10^{11} to 10^{7} m^{2}/V.s, (ζ) range -500 to 500 mV and Scattering Angle 15°. The samples were measured in diluted hexane solvent in a ratio of 1:30 v/v using one solvent resistant electrode (model BI-SREL, Brookhaven Instruments Corporation) and the measurements were conducted in triplicate at 25 ± 1 °C, the temperature was controlled and ranged from -5 °C to 110 °C, with active control, no external circulator was required. The interval between each reading cycle was 1 s, and the readings were obtained for a total of 20 cycles.

The thermochromic coatings were characterized before and after exposure to salt spray and thermodegradation by spectrophotometry to determine their ΔE. Coatings that had been exposed to photodegradation were characterized by spectrophotometry to determine their ΔE by Fourier transform infrared (FTIR) and UV-Vis spectroscopy, thermogravimetric analysis (TGA), and differential scanning calorimetry (DSC).

FTIR spectroscopy was performed using a Shimadzu IRAffinity-1S spectrophotometer (Kyoto, JP), and the interferograms were averaged over 24 scans at 2 cm^{-1} resolution and recorded from 4,000 to 400 cm^{-1} with KBr tablets.

Approximately 5 ± 1 mg of each sample was used for TGA. The analyses were performed using a Shimadzu's TGA-50 thermobalance (Kyoto, JP) under an inert N$_2$ atmosphere with a flow rate of 50 mL min^{-1} and heating rate of 10 °C min^{-1}; a Pt crucible as used as a sample holder. The maximum temperature was 900 °C.

Samples of approximately 2 ± 0.5 mg were analyzed using a Netzsch's DSC 3500 Sirius Calorimeter (Selb, DE) with MFC and IntraCooler40 measuring cell (gas tight) in

an inert N$_2$ atmosphere with a flow rate of 40 mL min^{-1}, purge gas with a flow rate of 60 mL min^{-1}, and heating rate of 10 °C min^{-1} using an crucible Concavus pan and lid from Al, outer bottom Ø 5 mm, with a capacity of 30/40 μL, cold weldable. The analyzes were conducted with heating from 25 °C to 130 °C at a rate of 10 ºC/min, keeping a constant temperature of 130 °C for 2 min followed by cooling down to 25 ºC. The second heating and cooling run was conducted with the same temperature intervals at a rate of 10 ºC/min.

UV-vis absorption spectroscopy was performed using Shimadzu UV2450PC spectrophotometer with an ISR-2200 integrating sphere attachment (Kyoto, JP). All experiments were performed at 25 °C. The baseline was obtained using BaSO$_4$ (Wako Pure Chemical Industries, Ltd.).

The total color difference (ΔE) was assessed using a KYK portable spectrophotometer from Gardner GmbH (Spectroguide Sphere Gloss 6834) with a D65 light source and an observation angle of 10°. The CIELAB measurement scale was used in this study. The colorimetric coordinates, L* (brightness), a* (green and red), and b* (blue and yellow), of each sensor were measured according to ASTM D2244[27]. Equation 1 was used to calculate ΔE .

$$\Delta E = \sqrt{\Delta L^2 + \Delta a^2 + \Delta b^2} \qquad (1)$$

where ΔL is the variation in luminosity between the test (after weathering) and standard (before weathering) samples, and Δa and Δb are the color variations between the test and standard samples. For all the parameters in Equation 1, the units of measurement are dimensionless.

3. Results and Discussion

3.1. Stability of the thermochromic dyes

Figure S1 shows photographs of YAP (a) and YAPMTP (b). All prepared dyes were stored for 30 days at room temperature. Separation or decantation was not observed during the study period.

This property ζ refers to the electrostatic potential in the shear plane of a particle, and can have positive, negative, or zero values. The greater the magnitude of ζ, the better the stability of the suspensions, owing to their lower tendency to agglomerate because of the repellency of charges with the same value[28]. The ζ values of YAP, YAPMTP, and YAPMTP-TiO$_2$ were measured on the day the paints were prepared and after 30 days and showed similar results. YAP showed ζ values of −27.7 ± 0.5 mV and 27.3 ± 0.5 mV, YAPMTP showed ζ values of −29.0 ± 1.4 mV and −28.0 ± 0.4 mV, and YAPMTP-TiO$_2$ showed ζ values of −32.7 ± 0.6 mV and −30.1 ± 1.6 mV. The addition of MTP and TiO$_2$ did not significantly alter the ζ of the coatings, and the variations within the 30-day interval were not significant. This indicates that the addition of MTP and TiO$_2$ did not alter the stability of the yellow alkyd paint. Moreover, highly negative or positive ζ values in the range of 30 mV or higher are typical of dispersions with good stability[29,30].

3.2. Initial colorimetric coordinates of the thermochromic coatings

The average values of the colorimetric coordinates of the thermochromic coatings before the artificial weathering tests are presented in Table 2. According to the a* (negative = green) and b* (positive = yellow) values obtained, all the coatings showed a greenish-yellow coloration. YAPMTP and YAPMTP-VL showed a low ΔE of 1.08. This variation was barely visible to the naked eye because the L*, a *, and b *values were very close. When TiO_2 was added to the paint mixture, a pronounced increase in ΔE compared to the standard samples was observed for YAPMTP-TiO_2 (2.32) and YAPMTP-VL-TiO_2 (3.11). This increase in ΔE is due to the fact that TiO_2 has the property of opacification given its refractive index. This property causes L* to increase. The addition of TiO_2 increased the intensity of the green coloration of the coatings, as indicated by the mean values of a*.

3.3. Thermodegradation resistance

The ANOVA (analysis of variance) results of the ΔE of the thermochromic sensors exposed to thermodegradation are shown in Table 3. An adjusted R^2 value of 0.819 was obtained at a 95% confidence level. TiO_2, ET, and their interaction showed a significant influence on the ΔE of thermochromic sensors exposed to thermodegradation ($p < 0.05$). TiO_2, ET, and the interaction TiO_2–ET showed F factor values of 31.182, 38.905, and 35.293, respectively, indicating that ET contributed the most to the color change of the thermochromic sensors during the thermodegradation test.

The largest ΔE of the thermochromic sensors under thermodegradation was observed after 480 h of exposure, as shown on the response surface in Figure 2. The statistical model of this response surface is provided in the Supplementary Material (Eq. S1).

When TiO_2 was added to the thermochromic paint, the resulting coating exhibited greater resistance to the effects of temperature. The ΔE values obtained for YAPMTP-TiO_2 and YAPMTP-VL-TiO_2 were equal to 1.46 and 1.30, respectively. The ΔE between these dyes was equal to 1.13; according to Zhu et al.[6], this value reflects on a slight change (0.5 – 1.5) in ΔE.

YAPMTP-VL showed a ΔE value of 2.85, which is higher than that obtained from YAPMTP (2.52). When the colors of YAPMTP and YAPMTP-VL were compared, the ΔE observed was equal to 3.84. According to Zhu et al.[6], a variation of Δ of this magnitude can be considered a distinguishable change (3.0 – 6.0) by the naked eye.

3.4. Resistance to salt spray

Table 4 shows the ANOVA results for the ΔE of the thermochromic coatings exposed to salt-spray conditions.
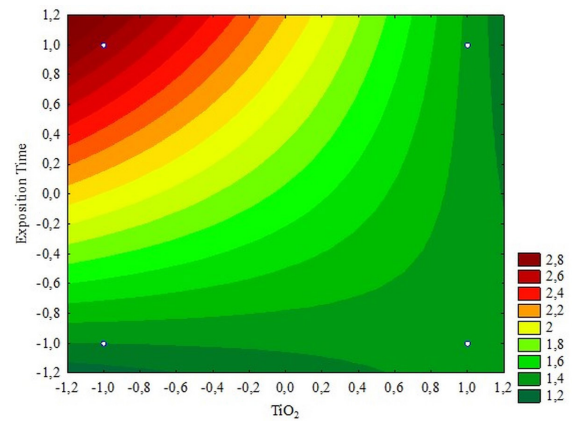

Figure 2. Color variation of the thermochromic sensors upon thermodegradation.

Table 2. Initial colorimetric coordinates of the thermochromic coatings.

Coatings	L*	a*	b*
YAPMTP	40.48 ± 0.07	-1.99 ± 0.08	18.66 ± 0.08
YAPMTP-VL	39.98 ± 0.19	-1.97 ± 0.10	19.61 ± 0.11
YAPMTP-TiO_2	42.68 ± 0.34	-2.66 ± 0.11	18.38 ± 0.79
YAPMTP-VL-TiO_2	43.55 ± 0.25	-2.49 ± 0.04	18.55 ± 0.47

Table 3. ANOVA results of the color variations of the thermochromic coatings under thermodegradation.

Factor	SS	df	MS	F	p
(1)	0.056	1	0.056	0.713	0.411
(2)	2.428	1	2.428	31.182	0.000
(3)	3.030	1	3.030	38.905	0.000
1 × 2	0.145	1	0.145	1.861	0.191
1 × 3	0.197	1	0.197	2.526	0.132
2 × 3	2.748	1	2.748	35.293	0.000
1 × 2 × 3	0.048	1	0.048	0.612	0.445
Error	1.246	16	0.078		
Total SS	9.897	23			

(1) VL; (2) TiO_2; (3) Exposure time Adj. $R^2 = 0.819$; $\alpha = 0.05$ SS – sum of squares; df – degree of freedom; MS – mean square; F – F-distribution; p – p value.

An adjusted R^2 value of 0.765 was obtained at a 95% confidence level. The factors TiO_2, VL, and ET, as well as the TiO_2–ET interaction, showed a significant influence on the ΔE of the thermochromic sensors when exposed to salt spray ($p < 0.05$). VL, TiO_2, and ET exhibited F-factors of 6.852, 10.467, and 20.965, respectively. The interaction TiO_2–ET showed the highest F factor (37.905). This result indicates the synergistic effects between the two factors, and their interaction contributed the most to the ΔE of the coatings during exposure to salt spray.

The interactions between VL and TiO_2 and between VL and ET did not show statistically significant differences. The response surfaces of the effects of TiO_2 and ET on the ΔE of the thermochromic sensors are shown in Figure 3. The equation for the statistical model is provided in Supplementary Material (Eq. S2).

TiO_2 addition decreased the ΔE of the thermochromic coatings, and the VL–TiO_2 interaction contributed to the decrease in ΔE. YAPMTP-TiO_2 and YAPMTP-VL-TiO_2 showed ΔE values equal to 1.51 and 1.15, respectively. The ΔE between these coatings was 1.13; according to Zhu et al.[6], a variation of ΔE of this magnitude means a slight change ($0.5 - 1.5$) in color. This change cannot be identified by the naked eye. Therefore, TiO_2 may provide greater colorimetric stability to coatings owing to its ability to reduce the diffusion of chemical agents. According to some researchers[31,32], TiO_2 particles decrease the permeability of coatings and delay the passage of corrosive ions and chemical agents that can react with the coating components and cause coloration changes. Wang et al.[33] added TiO_2 nanoparticles to epoxy coatings to improve their anticorrosive properties by decreasing the diffusion of chemical agents.

The ΔE of the sensors exposed to salt spray was similar to that obtained following exposure to temperature, indicating that temperature has a greater influence on ΔE than the diffusion of chemical agents in the salt spray test.

YAPMTP-VL showed a ΔE of 2.61 at an ET of 480 h, which is similar to its ΔE after the thermodegradation test. According to Zhu et al.[6], variations in ΔE of this magnitude are considered an appreciable change ($1.5 - 3.0$) by the naked eye.

3.5. Photodegradation resistance

The ANOVA results of the ΔE of the thermochromic sensors exposed to UV-A and UV-B radiation are shown in Table 5.
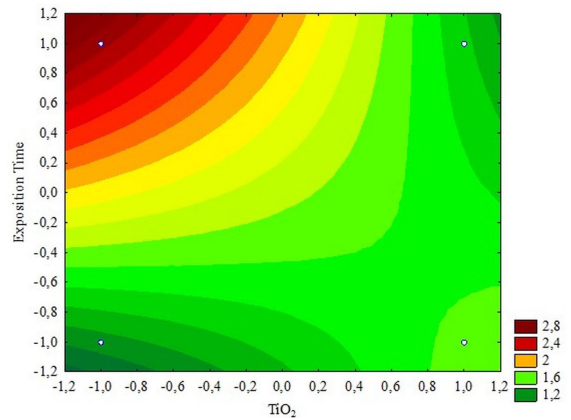

Figure 3. Color variation of the thermochromic sensors upon exposure to salt spray.

Table 4. ANOVA results of color variations under salt spray.

Factor	SS	df	MS	F	P
(1)	0.683	1	0.683	6.852	0.019
(2)	1.043	1	1.043	10.467	0.005
(3)	2.090	1	2.090	20.965	0.000
1*2	0.185	1	0.185	1.859	0.192
1*3	0.325	1	0.325	3.260	0.090
2*3	3.778	1	3.778	37.905	0.000
1*2*3	0.040	1	0.040	0.396	0.538
Error	1.595	16	0.100		
Total SS	9.740	23			

(1) VL; (2) TiO_2; (3) Exposure time Adj. $R^2 = 0.765$; $\alpha = 0.05$

Table 5. ANOVA results of the color variation of the thermochromic sensors under UV-A and UV-B exposure.

Factor	SS	df	MS	F	p
(1)	4.588	1	4.588	138.779	0.000
(2)	115.547	1	115.547	3495.129	0.000
(3)	162.380	1	162.380	4911.735	0.000
1 × 2	4.294	1	4.294	129.874	0.000
1 × 3	0.420	1	0.420	12.698	0.003
2 × 3	6.065	1	6.065	183.468	0.000
1 × 2 × 3	0.115	1	0.115	3.487	0.080
Error	0.529	16	0.033		
Total SS	293.938	23			

(1) VL; (2) TiO_2; (3) Exposure time Adj. $R^2 = 0.997$ $\alpha = 0.05$

An adjusted R^2 value of 0.997 was obtained at a 95% confidence level. The factors VL, TiO_2, and ET showed significant influences on the ΔE of the thermochromic sensors exposed to photodegradation ($p < 0.05$). However, the correlation of the interaction VL–TiO_2–ET had a p-value of 0.080, indicating no statistical significance.

The ET to UV-A and UV-B radiation was the factor that contributed the most to the increase in ΔE of the thermochromic coatings, regardless of the type of protection applied; this factor had an F factor of ~4912. The F factors of TiO_2 and the VL were ~3495 ~ and 139, respectively.

The ΔE of all thermochromic coatings changed continuously with ET, as shown in Figure 4, and the ΔE tended to increase at a lower rate under longer ETs. This finding is related to the degradation of the thermochromic leuco dye added to the base paint because this type of leuco dye is susceptible to photodegradation[21]. By contrast, when one of the protective agents was present in the coating, the rate of increase in ΔE imposed by UV-A and UV-B radiation decreased. TiO_2 contributes the most to minimizing the rate of increase in ΔE. TiO_2 is a semiconductor with a band gap of 3.0 eV; thus, it can absorb most of the UV radiation and effectively protect the organic polymers in the coating[34].

When ANOVA was performed to assess the effects of VL–TiO_2 and VL–ET, no significant differences were observed (Tables S1 and S2). The response surface plots presented in Figures 5 show the effect of TiO_2 and ET on the ΔE of the thermochromic sensors subjected to UV-A and UV-B exposure. The statistical model of the response surface is expressed by Eq. S3 in the Supplementary Material. The ΔE s of YAPMTP at ETs of 240 and 480 h were 14.57 and 20.90, respectively. The ΔE between these times was 6.36, which is much higher than that obtained for the thermodegradation and salt spray conditions. This ΔE could be classified as an obvious color change (6.0 – 12.0), according to Zhu et al.[6]; that is, the variation is easily observed by the naked eye. Therefore, this thermochromic film is highly sensitive to UV-A and UV-B radiation because leuco dyes are susceptible to photodegradation[21].

The addition of VL as a protective layer over the thermochromic film reduced the ΔE of the sensors by ~9%. However, the addition of TiO_2 led to a reduction in ΔE of ~30% under both ETs, corresponding to ΔE values of 10.2 and 14.8 for ETs at 240 and 480 h, respectively. The influence of ET on photodegradation was evidenced by the ΔE (4.77) obtained for the coatings doped with TiO_2 only. According to Zhu et al. (2017)[6], this variation was highly noticeable (> 12.0) to the naked eye (> 12.0).

The colorimetric coordinates, L*, a*, and b*, were assessed using ANOVA. L* showed a variation of approximately four points in all experiments. The effects of VL, TiO_2, and ET on this coordinate yielded an adjusted R^2 value of 0.992 (Table S3). All the factors analyzed contributed to an increase in the brightness of the paint color, with ET being the most responsible for this change (F factor, ~2636). The addition of TiO_2 to the paint contributed to a 23% reduction in the variation in this coordinate between the two exposure times. However, when ANOVA was performed to assess the effects of the interactions between VL and ET and TiO_2–ET, VL and TiO_2 appeared to be non-significant factors affecting the color brightness of the thermochromic sensors.
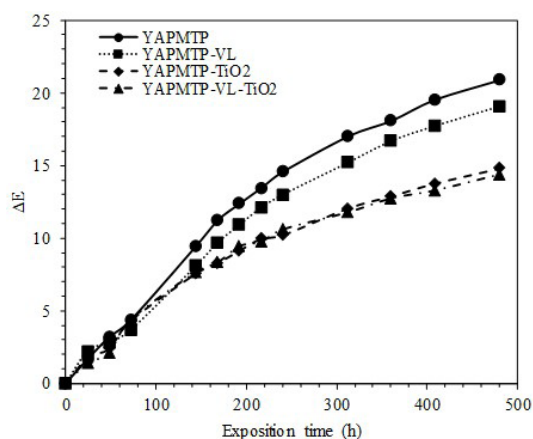

Figure 4. Effect of exposure time on the color variation of the thermochromic sensors.
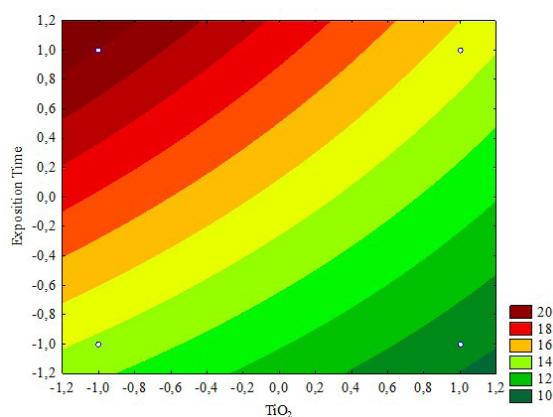

Figure 5. Color variations of the thermochromic sensors under UV-A and UV-B exposure.

These findings confirm that ET was the factor that most significantly altered this parameter. The average plots for the L* coordinates are shown in Figures S2(a) and S2(b).

The colorimetric coordinate a* showed a variation of ~3 points within the positive range of the scale corresponding to red (+). According to the ANOVA results presented in Table S4, the adjusted R^2 value is 0.999. All factors and their interactions contributed to statistically significant changes in the values of this coordinate ($p < 0.05$). TiO_2 contributed the most to the decrease in the value of a* (F factor = ~18745), whereas ET (F factor = ~1413) and VL (F factor = ~725) contributed to the increase in the value of this coordinate. The addition of TiO_2 to the paint reduced the intensity of the red color present in the paint by ~93% between the two ETs. This may be associated with the protective effects of TiO_2 against UV irradiation. The response surfaces for this coordinate system are shown in Figures S3(a) and S3(b), and the mathematical model is given in Eq. S4.

The b* coordinates exhibit the greatest variation, corresponding to ~ nine points within the positive axis of the coordinates. The ANOVA showed an adjusted R^2 value of 0.999 for the effects of the factors analyzed on b*, as shown in Table S5. TiO_2 contributed the most to the decrease in

b* (F factor, ~13371), whereas ET contributed the most to the increase in the values of this coordinate (F factor, ~19564). The VL contributed to a decrease in b* (F factor, ~322). However, in terms of magnitude, the effect was much less than that of TiO_2. All factors and their interactions were statistically significant (p < 0.05) for b *behavior. TiO_2 decreased the variation of b* by ~24%; however, ET increased the value of this coordinate by ~16%. Exposure of the thermochromic dye to UV-A and UV-B rays for long periods increased film yellowing. The variation in b* affects the L* brightness of the dye. This yellowing can be explained by the degradation of the alkyd resin present in the base dye used in this study[35], which is similar to the degradation of the thermochromic leuco dye under UV radiation, as determined by Lötzsch and Seeboth[21]. TiO_2 can help reduce this effect in thermochromic dyes. The responses of b* were verified on the response surfaces shown in Figures S4(a) and S4(b), and the mathematical model given by Eq. S5.

Among the weathering conditions studied, the thermochromic sensors exhibited the greatest sensitivity to UV-A and UV-B radiation. Therefore, the sensors were subjected to further investigation using UV-vis spectroscopy, FTIR, TGA, and DSC to identify the structural changes in the thermochromic paints.

3.5.1. FTIR spectroscopy

Figure 6 shows the FTIR spectra of the sensors applied only with the thermochromic paint (YAPMTP), which does not contain VL and TiO_2, and exposed to UV-A and UV-B radiation for 0, 240, and 480 h. The disappearance of bands and the emergence of new peaks related to homolytic bond breaking were not observed in the spectra. Moreover, reductions in the intensity of the peaks attributed to the O–H stretching of hydroxyl groups between 3400 cm^{-1} and 3200 cm^{-1}, axial deformation of C-H groups (alkyd and aromatic) at 2920 cm^{-1} and 2840 cm^{-1}, angular deformation of CH_2 groups at 1452 cm^{-1}, and angular deformation of the C-O bonds of alcohols were not observed.

The degradation of organic compounds containing the carbonyl group –C=O, such as carboxylic acids and esters, is usually accompanied by variations in the intensity of the peak at ~1720 cm^{-1} owing to changes in the stretching vibrations of this functional group[24,36]. In this study, no significant variations in this region of the FTIR spectrum were observed.

Prolonged exposure to UV-A and UV-B radiation did not degrade the structures of the thermochromic coatings to an extent that could be assessed using FTIR. Very small variations in the polymer chains were difficult to detect using FTIR spectroscopy. This behavior was also observed when VL, TiO_2, or both were added to the thermochromic paint (Figure S5).

3.5.2. UV-Vis Spectroscopy

The effect of exposure to UV light (UV-A and UV-B) was analyzed using UV-vis absorption spectroscopy, and the results are shown in Figure 7. YAPMTP, YAPMTP-VL, YAPMTP-TiO_2, and YAPMTP-VL-TiO_2 did not show significant variations in their absorption bands. However, when exposed to UV light, reductions in the absorption intensity were observed in the 500–700 nm region, and these reductions became more significant with increasing exposure time. This change in the UV-vis absorption spectra indicates alterations in the chemical structures of the coatings owing to UV light exposure.

The changes in the absorption of YAPMTP and YAPMTP-VL were more significant than those of YAPMTP-TiO_2 and YAPMTP-VL-TiO_2. Moreover, the coatings with added TiO_2 exhibited less variation in the intensity of their absorption at exposure times of 240 and 480 h. As previously mentioned, TiO_2 protects polymers against UV-A and UV-B radiation[24].

3.5.3. TGA and DSC

The samples were assessed by TGA and DSC without (0 h) and with (240 and 480 h) exposure to UV-A and UV-B radiation. The TGA curves indicated that the samples did not exhibit significant changes in the maximum degradation temperature (T_{deg}), and the DSC analyses revealed that the melting temperature of the system (T_m) did not exhibit significant variations. The TGA and DSC results are summarized in Table 6 and the corresponding curves are shown in Figures S6 and S7, respectively. The melting peak at 65 °C reflected the occurrence of a phase transition; at temperatures above 65 °C, the leuco dye became colorless.
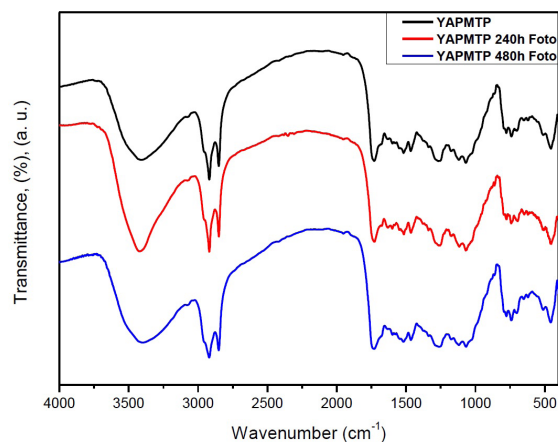

Figure 6. FTIR spectra of thermochromic sensors without VL and TiO_2 under UV-A and UV-B radiation: (a) No exposure, b) 240 h, and c) 480 h.

Table 6. Thermal properties of standard and experimental samples before and after UV-A and UV-B exposure.

Samples	T_{deg1} (°C)	T_{deg2} (°C)	T_m (°C)
MTP	365	-	65
YAP	405	457	-
YAPMTP	403	454	65
YAPMTP 240h	402	454	65
YAPMTP 480h	402	457	65

(I) T_{deg1}: first-stage degradation temperature; (II) T_{deg2}: second-stage degradation temperature; (III) T_m: fusion temperature of the system.

The T_m was mainly influenced by the solvent present in the microencapsulated thermochromic pigment[37]. The color transition temperatures of the coatings did not change, despite the color change. Thus, the sensors maintained their ability to detect temperature variations.

Figure 8 present one summary for paint and reversible thermochromic coating preparation. When the temperature of the surface of the substrates on which the coatings were applied was increased to 65 °C, shows the color changes of the thermochromic substrate.
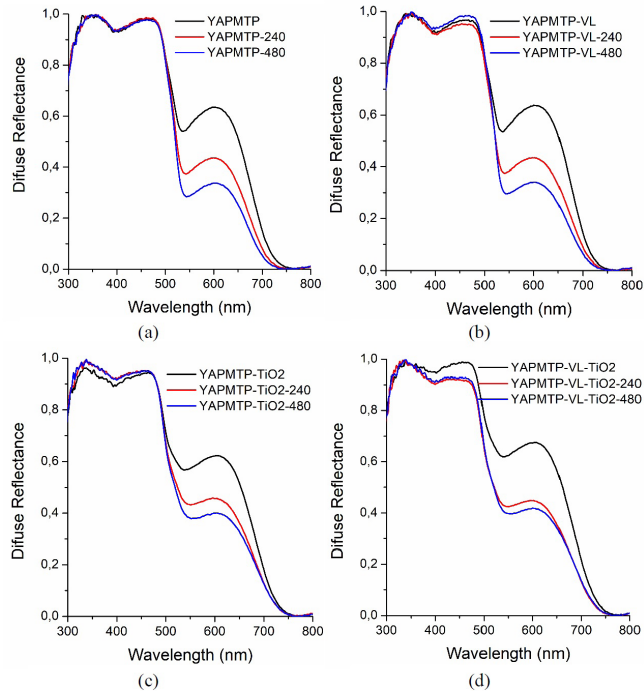

Figure 7. UV-vis absorption spectra of the thermochromic coatings (a) YAPMTP, (b) YAPMTP-VL (c) YAPMTP-TiO$_2$, and (d) YAPMTP-VL-TiO$_2$ without (0 h) and with (240 h and 480 h) exposure to UV-A and UV-B radiation.
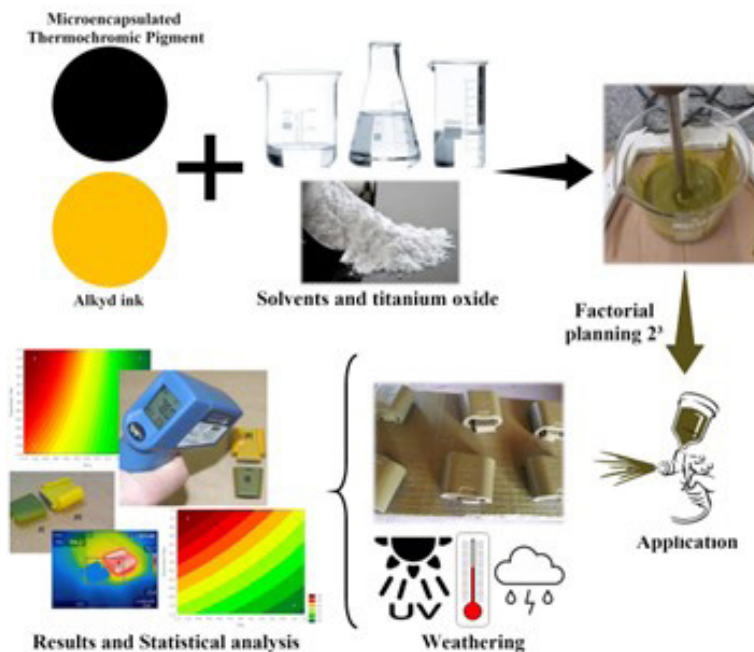

Figure 8. Schematic diagram for fabrication thermochromic, coatings used as sensors to protect electricity distribution systems.

4. Conclusion

In this study, thermochromic coatings composed of a microencapsulated thermochromic pigment mixed with an alkyd paint were developed for use as thermal sensors. The resistances of the sensors to thermodegradation, salt spraying, and photodegradation were also investigated.

The results of color-change assessments performed on the thermochromic sensors indicated that thermal weathering and salt spraying had little impact on the color of the sensors. Photodegradation is a weathering condition that alters the color of sensors the most.

TiO_2 was added to the thermochromic paints to increase the resistance of the sensors to weathering, especially photodegradation, and VL was applied to the thermochromic coatings. TiO_2 has proven to be an interesting alternative to other compounds used to increase the photodegradation resistance of thermochromic coatings prepared using leucopigments from the fluoran family by acting as a physical radiation blocker. The use of chemical blockers such as VL did not change the photodegradation resistance of the thermochromic coatings.

The better photodegradation resistance results obtained with the addition of TiO_2 to the paint composition are promising. The increased color stability of paints containing leuco pigments from the fluoran family allows thermosensors to be applied in external environments.

There is still a need for further investigations with TiO_2, such as increased concentration, different crystalline structures, and different particle sizes, with the aim of further increasing photodegradation resistance.

The use of reversible thermochromic coatings has been developed and applied in the form of paint, adhesive labels, varnishes, sprays, or the addition of pigment powder in polymers. The masterbatch can be easily processed by conventional technologies such as extrusion, injection during the coating of parts, equipment, insulators, electric cable covering, switches, sockets, ceiling lamp nozzles, parts for automotive cooling systems, and plastic combustion engine protectors, fairings, and can increase the detection speed of hot spots and preventive maintenance in electrical connections. The most important finding is that the thermal device developed helps to monitor with naked eye places where heating above normal levels is present, corroborating its potential to facilitate the identification of potential failure points in electrical energy distribution systems and/or other industrial processes where there is a requirement for temperature control, without the need for other equipment or direct and indirect methods, such as thermographic cameras, thermocouples, immersion, contact and infrared thermometers.

In recent studies Souza et al.[38], synthesized and characterized vanadium dioxide (VO_2) nanostructures with progressive thermochromic properties by hydrothermal methods, favoring a 22% reduction in the MIT temperature (metal-insulator transition) and in another study Duarte et al.[39] they presented new classes of spiropyran and merocyanine that can possess changing color properties under UV and visible light and temperature fluctuations[38,39]. The results obtained show favorable potential applications in intelligent materials, such as identification ink, safety indicators in the petrochemical industry, smart windows, memory storage devices, food safety, research engineering, aerospace, gas vapor sensors, dyes for solar cells, other luminescent switches of solid-state materials, sportswear for the detection of physical exhaustion and/or management of lab-on-a-chip technologies, and finally thermal mapping used in biomedical sciences.

6. References

1. Braunovic M, Myshkin NK, Konchits VV. Electrical contacts: fundamentals, applications and technology. Boca Raton: CRC Press; 2007. https://doi.org/10.1201/9780849391088.
2. Oldoni CR. Estudo e caracterização de contaminantes em isoladores de regiões rurais [Dissertação]. Blumenau: Universidade Regional de Blumenau; 2009.
3. McGrath MJ, Scanaill CN. Sensor technologies: healthcare, wellness and environmental applications. New York: ApressOpen; 2013. Sensing and sensor fundamentals; p. 15-50.
4. Akishino JK, Cerqueira DP, Silva GC, Swinka-Filho V, Munaro M. Morphological and thermal evaluation of blends of polyethylene wax and paraffin. Thermochim Acta. 2016;626:9-12.
5. Lindquist, TM, Bertling, L, Eriksson, R. Estimation of disconnector contact condition for modeling the effect of maintenance and ageing. In: IEEE Russia Power Tech; June 2005; St. Petersburg, Russia. Proceedings. USA: IEEE; 2005.
6. Zhu X, Liu Y, Dong N, Li Z. Fabrication and characterization of reversible thermochromic wood veneers. Sci Rep. 2017;7(16933):1-10.
7. Kulčar R, Friškovec M, Hauptman N, Vesel A, Gunde MK. Colorimetric properties of reversible thermochromic printing inks. Dyes Pigm. 2010;86(3):271-7.
8. MacLaren DC, White MA. Competition between dye–developer and solvent–developer interactions in a reversible thermochromic system. J Mater Chem. 2003;13(7):1701-4.
9. He Y, Li W, Han N, Wang J, Zhang X. Facile flexible reversible thermochromic membranes based on micro/nanoencapsulated phase change materials for wearable temperature sensor. Appl Energy. 2019;247:615-29.
10. Zhu CF, Wu AB. Studies on the synthesis and thermochromic properties of Crystal violet lactone and its reversible thermochromic complexes. Thermochim Acta. 2005;425(1-2):7-12.
11. Özkayalar S, Adigüzel E, Aksoy SA, Alkan C. Reversible color-changing and thermal-energy storing nanocapsules of three-component thermochromic dyes. Mater Chem Phys. 2020;252:1-12.
12. Seeboth A, Lötzsch D, Potechius E, Vetter R. Thermochromic effects of leuco dyes studied in polypropylene. Chin J Polym Sci. 2006;24(4):363-8.
13. Geng X, Li W, Wang Y, Lu J, Wang J, Wang N, et al. Reversible thermochromic microencapsulated phase change materials for thermal energy storage application in thermal protective clothing. Appl Energy. 2018;217:281-94.
14. Muthyala R. Chemistry and applications of leuco dyes. New York: Springer; 2002.
15. Geng X, Gao Y, Wang N, Han N, Zhang X, Li W. Intelligent adjustment of light-to-thermal energy conversion efficiency of thermo-regulated fabric containing reversible thermochromic MicroPCMs. Chem Eng J. 2021;408:1-16.
16. Burkinshaw SM, Griffiths J, Towns AD. Reversibly thermochromic systems based on pH-sensitive functional dyes. J Mater Chem. 1998;8(12):2677-83.

17. Cesconeto RB, Rodrigues A, Dal-Bó AG, Dias NL Fo, Rocha MR, Frizon TEA. Evaluation of a thermochromic liquid crystal for use as a temperature sensor for components of electrical systems. Mater Res. 2017;20(2):130-6.

18. Singh B, Sharma N. Mechanistic implications of plastic degradation. Polym Degrad Stabil. 2008;93(3):561-84.

19. Wojciechowski K, Skowera E, Pietniewicz E, Zukowska GZ, van der Ven LGJ, Korczagin I, et al. UV stability of polymeric binder films used in waterborne facade paints. Prog Org Coat. 2014;77(2):298-304.

20. Wicks ZW, Jones FN, Pappas SP, Wicks DA. Organic coatings: science and technology. 3rd ed. New Jersey: John Wiley & Sons; 2006.

21. Seeboth A, Lötzsch D. Thermochromic phenomena in polymers. Minnesota: Smithers Rapra; 2008.

22. Yanagita M, Takahashi S, Aoki I. Development of high lightfast fluoranleucodyes for thermosensitive recording papers. J. Jap. Soc. Col. Mater. 1996;69:649-57.

23. Oda H. New developments in the stabilization of leuco dyes: effect of UV absorbers containing an amphoteric counter-ion moiety on the light fastness of color formers. Dyes Pigm. 2005;66(2):103-8.

24. Wojciechowski K, Zukowska GZ, Korczagin I, Malanowski P. Effect of TiO_2 on UV stability of polymeric binder films used in waterborne facade paints. Prog Org Coat. 2015;85:123-30.

25. ASTM: American Society for Testing and Materials. ASTM B117-19: standard practice for operating salt spray (Fog) apparatus. West Conshohocken: ASTM; 2019.

26. ASTM: American Society for Testing and Materials. ASTM G154-16: standard practice for operating fluorescent ultraviolet (UV) Lamp Apparatus for exposure of nonmetallic materials. West Conshohocken: ASTM; 2016.

27. ASTM: American Society for Testing and Materials. ASTM D2244-21: standard practice for calculation of color tolerances and color differences from instrumentally measured color coordinates. West Conshohocken: ASTM; 2021.

28. Karakaş F, Çelik MS. Stabilization mechanism of main paint pigments. Prog Org Coat. 2018;123:292-8.

29. Mandzy N, Grulke E, Druffel T. Breakage of TiO_2 agglomerates in electrostatically stabilized aqueous dispersions. Powder Technol. 2005;160(2):121-6.

30. Costa JRC, Correia C, Góis JR, Silva SMC, Antunes FE, Moniz J, et al. Efficient dispersion of TiO_2 using tailor made poly (acrylic acid) − based block copolymers, and its incorporation in water based paint formulation. Prog Org Coat. 2017;104:34-32.

31. Deyab MA, Nada AA, Hamdy A. Comparative study on the corrosion and mechanical properties of nano-composite coatings incorporated with TiO_2 nano-particles, TiO_2 nano-tubes, and ZnO nano-flowers. Prog Org Coat. 2017;105:245-51.

32. Sørensen PA, Kiil S, Dam-Johansen K. Anticorrosive coatings: a review. J Coat Technol Res. 2009;6:135-76.

33. Wang N, Fu W, Zhang J, Li X, Fang Q. Corrosion performance of waterborne epoxy coatings containing polyethylenimine treated mesoporous-TiO_2 nanoparticles on mild steel. Prog Org Coat. 2015;89:114-22.

34. Löf D, Hamieau G, Zalich M, Ducher P, Kynde S, Midtgaard SR, et al. Dispersion state of TiO_2 pigment particles studied by ultra-small-angle X-ray scattering revealing dependence on dispersant but limited change during drying of paint coating. Prog Org Coat. 2020;142:1-8.

35. Fazenda JMR. Tintas e vernizes: ciência e tecnologia. 3. ed. São Paulo: Editora Edgard Blücher; 2005.

36. Lopes F, Neves J, Campos A, Hrdina R. Weathering of microencapsulated thermochromic pigments. Res J Text. Apparel. 2009;13(1):78-89.

37. Panák O, Držková M, Kaplanová M, Novak U, Gunde MK. The relation between colour and structural changes in thermochromic systems comprising crystal violet lactone, bisphenol A, and tetradecanol. Dyes Pigm. 2017;136:382-9.

38. Souza AM, Cercena R, Duarte RC, Arcaro S, Dal Bó AG. The influence of precursors and additives on the hydrothermal synthesis of VO_2: a route for tuning the metal–insulator transition temperature. Ceram Int. 2020;46(1):23560-6.

39. Duarte RC, Silveira F, Bercini AB, Cercena R, Brondani D, Zapp E, et al. Synthesis of a 5-carboxy indole-based spiropyran fluorophore: thermal, electrochemical, photophysical and bovine serum albumin interaction investigations. Chemos. 2020;8:31.

Supplementary material

The following online material is available for this article:

Supplementary material.